xIlkogretim Online - Elementary Education Online,2021; Vol 20 (Issue 1): pp.2314-2326
http://ilkogretim-online.org
doi: 10.17051/ilkonline.2021.01.258

An Early Prediction of Lung Cancer and its Classification through Measurement of Physical Characteristics using CT Scan Images

K.Karthika, Research Scholar Department of ECE, VISTAS, Chennai, India. karthikakaliapan@gmail.com
G.R.Jothilakshmi, Associate Professor Department of ECE, VISTAS, Chennai, India. jothi.se@velsuniv.ac.in

Abstract- Lung tumor is a general happening nature in a people and solitary among lethal cancers. Recently, out of a number of researches presented by diverse health agencies, it is obvious with the purpose of the casualty percentage is going up due to postponed finding of lung cancer. Hence, an synthetic intellect base finding is compulsory to locate out the beginning of lung bump micro-calcification, which might bear the health center and radiologists to correctly expect it during figure dispensation method. In this document, a narrative practice is planned to classify the strike micro-calcification model by means of its material features. The corporeal facial appearance that full into report are the reflection coefficients and mass densities of the binned CT image of lung. The physical features measurements reiterate once again the existence of malignant nodule. Then, by applying the method of thresholding and in interruption of bodily skin tone, a three-dimensional (3D) expected representation of the section of concern (ROI) is achieve in esteem of material dimensions. Thus, the lump extent is planned from mains protuberance.

This idea is worn to bear out how best in categorization with 100 wicked imagery (the protuberance presence) and 10 usual imagery (the lump absence). Apart extent measurement, the planned process ropes SVM classifier to take steps for brilliant organization from ordinary and wicked enter imagery by presently by means of two corporeal facial appearance. The classifier exhibit an exactness of 98%.

Keywords: Lung cancer, CT image, micro-calcification, indication coefficient, group concentration, hankie impedance

I. INTRODUCTION

Indian committee of medicinal study (ICMR) probable that the nation (India) is credible to trace in excess of 17 lakh original tumor suitcases and more than 8 lakh malignancy death by 2020 [1]. Lung malignancy is happening to be chief motive for demise in together gender with an inference of 25.5 %. The likelihood of living wage for 5 times can appreciably pick up to 54% when the malignancy is branded at an original segment [2]. Still, the ability of alive can be enhanced to 18% for the patients detect with abundant urbanized growth [3]. The countrywide Lung transmission audition statement avowed that employ CT examine in malignancy finding resulted 20% diminish in demise charge due to pulmonary disease [4].

In all-purpose, the pulmonary nodules and micro-calcifications are often categorize base on round dense body with borders of parenchyma laceration, quantify with distance of fewer 3cm [5]. Though, not each pulmonary nodules and micro-calcifications are destructive (depict in fig 1). quite a lot of minuscule lump opacities may pull the wool over your eyes the nodules, purposely when single examine in a solitary dimensional plane, though they are feature [6], admirable on numerous flat surface imagery like two-dimension consistent dense lump, lesion, protect like atelectasis or respiratory area anomaly. In checkup care, mainframe Tomography (CT) takes on top of be highly approachable and celebrated imaging method for detect and diagnose the protuberance with comparative virtues on spatial resolution, expense, dominance and noninvasiveness [7]. CT is the moderately proficient procedure to distinguish the pulmonary protuberance and micro-calcifications since of its probable to produce 3 measurement descriptions of trunk crater, produce descriptions of nodules, micro-calcifications and pathological growth at elevated decision [8]. A figure of CT check through workstation process in regulate to carry opinion of pulmonary bump has been expansively engaged in hospitals. The radiologists want to revise a mixture of uniqueness specifically size, location, surface and figure etc. of the nodules and micro-calcifications from CT examine descriptions to complete diagnose job. At rest, this is rather dreadful and difficult, since quite a few constraints, that are misconception, complete together with controlled practice professionally.

Presently, the controlling process in order to spot and review the situation of pulmonary bump and micro-calcification would be biopsy technique; still this procedure is mostly persistent system that implicated withdrawal of hankie illustration honestly from the nodules and micro-calcifications. With immediately remove a little bump and micro-calcification fraction cannot stand for absolute individuality of the lump precisely since of its assorted features. Hence, complicated computer-assisted judgment base system will be requisite to hold radiologists to cope these problems, by interpret the facts of analysis to get a number of health check actions. The major anomaly linked to lung is nodules and calcifications from practitioner's

point of view. Nodules are unsusceptible in assessment with calcifications. There are two types of calcifications, one as worldwide and other as micro-calcification. Macro-calcifications [4] measured to be vast calcium evidence in the lung tissue, urbanized due to numerous factors. But, less important calcium statement stemmed micro-calcifications, in the lung hankie source the extremely disposed to extend cancer.

A. Extraction Methods of Image Details

Separately the occurrence of numerous nodules and micro-calcifications, fastidious lump and micro-calcification skin texture that decide capability of recognition surround their sizes, shapes, densities, marginalization, site and connection to yacht or pleural system [9]. Association with the surface of vascular or pleural structure heightens the probability of non-detection and false impression of pleural inflammation or damages [10]. Miniature in sufficiently strong-minded small concentration nodules and micro-calcification in chief site are more and more convoluted to perceive on compare with exterior superior nodules and micro-calcifications glowing marginalized scars [11].

The understanding of discovery of marginal nodules and micro-calcifications was condensed to partial in assessment with recognition of marginal nodules [9]. This marginal bump and micro-calcification imperceptibility enhanced the sympathy in small value.

The gratitude and organization of little blob of lung nodules and micro-calcifications from radiological descriptions of thoracic hollow are common challenge [12]. The reduce in casualty due to lung growth that prove for wider receipt of assessment of lung growth has harassed [13], they require for classification and evaluation of lump [14]. Accurate finding of considerable nodules and micro-calcifications is a precondition that is enhanced on training which used as a technique for computer-assisted detection [15]. Subsequently, the features of detected nodules and micro-calcifications display a basic difference. Nodules and micro-calcifications that detect are assessing through estimate by radiology mainly found on their shape and sizes.

B. Pattern Recognition

Numerous picture dispensation methods are useful to notice micro-calcification and categorize the tumor into kind and growth with the facial appearance of surface and shape. A widespread publication evaluation demonstrate that conventional technique in finding and categorization of micro-calcification include improvement [16], accompany by segmentation [17], after that removal of skin [20], and lastly the organization [21]. The imagery of CT and attractive character imaging (MRI) are working in finding of lung cancer. Initially, the X-ray descriptions are regard as a major exploratory technique to recognize any lung anomaly, especially lung cancer. X-ray is also a kind of non-intrusive process with the payment of organism fewer expense, instance saving, and superior accuracy. The expansion of model gratitude in figure dispensation requires being obtainable in a expedient method to hold the practitioner for right away suggestive of the vital desired direction to the patients regarding region of concern [18]. This document suggests a unite the mold gratitude connected to micro-calcification and current picture dispensation technique to supply a suitable process to a checkup practitioner. The optional method applies a tale technique to guess the micro-calcification region dimension by scheming the corporeal facial appearance of the standard micro-calcification in imagery [19]. In order to extract the abrasion corporal skin texture in the images, firstly, the bin of effort descriptions will be performed. The technique of bin crack an illustration into original than little sub-images, and this is deliberately helpful to achieve seal to the spoiled province and furthermore bring away evaluation now on the selected associate image. The thought of bin is very much useful to revise naval similes and now in this manuscript, this thought is fetch and functional to examine checkup descriptions to charge micro-calcification region amount. Further, the indication coefficient and group concentration computation from lung CT or MRI metaphors utilize figure dispensation process which is entirely infrequent procedure and adopt as a explore device here.

It is predominantly painstaking at this time the lung CT descriptions to categorize the occurrence of micro-calcification. A minuscule calcium authentication that extends in a few methods which develop into tumor is term as micro-calcification. Such calcification is separated into benevolent and wicked base on its outline, mass, borders, and extend, and the continuation of calcium composite. As an model, the benevolent tumor is classically owed to calcium oxalate, while disease is owed to calcium phosphate. From journalism investigation, it is found that micro-calcification is one of the main factors that may lead to some cancerous issues. Its identification within commencement and suitable description to medicos shall be to a great extent valuable for exploratory its outline, amount, and allotment of the calcium oxalate or calcium phosphate). The micro-calcification appear to be radiant colorless speck. The concentration of

micro-calcification is outweighing the concentration of extra zone in the lung representation. It is indispensable to sense the micro-calcification as province of curiosity (ROI). This is attaining by applying representation giving out method to recognize the scratch from additional tissues. Recognize the prototype of the scratch is necessary for deeper examination and categorization of anomaly that occur in lungs.

The technique of recognize prototype is additional obliging in categorization of the representation facial appearance on the foundation of commonalities in attendance in a few appearance. For identify the example connected to scratch, its interrelated facial appearance are to be obtained. Frequently, a number of segmentation methods are practical to notice the ROI. In improvement of the descriptions, the familiar functional method is the middle min–be very successful Gabor and Weiner filters. Conventional CT or MRI descriptions are vague impression with clatter and small distinction. Representation improvement is necessary to give emphasis to scrupulous uniqueness in attendance in descriptions. Thresholding outline and region-detection are the frequent technique functional while segmenting the descriptions. Segmentation takes on involved ingredient in ROI recognition. From detect ROI, characteristic figures are obtained through apply k resources and downy c-means cluster and SVM cluster to catalog on the source of, predictable model.

II. BACKGROUND AND APPROACH

The recommended practice is cooperative to recognize the micro-calcification outline in the figure, which vary from accessible conventional method of prototype acknowledgment. Here, the micro-calcification prototype is resolute from its corporal skin tone. The corporal facial appearance that in use into description are the gathering density and manifestation coefficients of protuberance section in CT or MRI descriptions. The recognized prototype of micro-calcification is represented in 3D picture form to conclude the figure and the amount of micro-calcification. The optional system comprises 9 stages and they are discussed elaborately below

A. Image Extraction

The Figure 1 shows the CT lung descriptions are extracted from Lung CT judgment dataset obtained from "The malignancy imaging documentation (TCIA)" They consisted standard as fine as difference (attendance of nodules) descriptions. The nodules of benevolent and cancerous (tumor) were described as grouping of difference descriptions. Irregularity descriptions are downloaded and functional for the examination at this time. Hundred descriptions are selected from Lung CT judgment, every 512 × 512 proportions. Protuberance location of each examine is downloaded as Representative-Tumor-Slices surpass from the equal location which describe the bump location in conditions of representation occurrence digit and x, y, z positions. Fig 1depicts the descriptions of ordinary and wicked bump difference occurrence. The intensities correlated to the variance locale are pretty elevated and it is revealed with ruby spherical smudge, and it is lumped micro-calcification seems to be incandescent sallow bad skin inside ROI.

Figure 1. (a) Normal Lung CT Image

(b) Malignant Lung CT Image

B. Binning the Images

The absolute lung CT representation is binned at initial into 3 rows and 4 columns. The foundation in select the bulk of matrix of every holder is described under:

1. The imagery that are binned ought to be the same in size

2. When the entire CT picture is bin with a number of sizes of rows and columns, then every primary stage bin representation dimension will be decreased. By asset of micro-calcification facial appearance, it might be teller into quite a few binned descriptions. Therefore, numerous binned metaphors require to be deliberate at next stage of bin in organize to take out the figure and mass of the micro-calcification.

3. When complete CT representation is bin with a smaller amount numeral of rows and columns, the binned figure will be of better amount. Consequently, undesired inappropriate workings could there collectively with micro-calcification lump. For this reason, binning at foremost point is performing with 3 rows and 4 columns as it is apposite for analysis.

The contribution representation dimension is 512 × 512 and resized it into 512×504 and it is depicted in Figure 2(a). This representation is preprocessed to take away external beam cage since its attendance has no sense. The beam confine naked picture is depicting in Figure 2(c). This preprocessing is approved elsewhere by means of segmentation procedure for extract thoracic hollow space and it is depict in Figure 2 (b). Following primary stage of bin, every bin picture will be of dimension 128 × 168 and it is depict in Figure 3. The storage bin that consists ROI is marked and places it for supplementary bin with 3 rows and 4 columns. Subsequent to next stage bin, the storage bin has its dimension of 64 × 84 as depict in Figure 4.

C. Reflection Co-Efficient

In lung tissues, a protuberance cancerous enlargement (micro-calcification) is urbanized due to calcium depositions. If contaminated lung with such irregularity place under scan, the lacerate body reflect additional power. For that reason, it is probable to work out the mirror image coefficient for the complete picture counting the scratch fraction. In the graze fraction, the reflect power and mirror image coefficient are together elevated. A picture could be model as a two-dimensional purpose $\mathbf{f}(x, y)$ with two mechanisms as

$$\mathbf{f}(x, y) = \mathbf{r}(x, y)\mathbf{i}(x, y) \qquad (1.1)$$

Where $\mathbf{i}(x, y)$ is the enlightenment constituent and $\mathbf{r}(x, y)$is the reflectance module.

$0 < \mathbf{i}(x, y) < \infty, 0 < \mathbf{r}(x, y) < 1$, $\mathbf{r} = 0$ represent whole assimilation, and $\mathbf{r} = 1$ represent whole reflectance.

Indication coefficient by means of curvature appropriate of smallest amount four-sided figure technique.
Just the once choose the appropriate storage bin that contain lump from subsequent stage of bin, in organize to notice ROI, it is required to appraise the manifestation coefficients for situation the entrance. The indication coefficients for every chain are graphed then on the subject of the individual paragraph morals of storage bin on x league and the broaden of the mirror image coefficients on y alliance. For ROI detect bin representation, it is probable to create elsewhere 42 mirror image coefficient graph (for a number of the rows are depict as crimson procession in Figures. 6, 7, 8, and 9). The accurate mirror image coefficient assortment that operates as doorstep in ROI uncovering is strong-minded by means of curvature appropriate of smallest amount four-sided figure (depict as cobalt column in the Figures. 6, 7, 8, and 9) and it is experiential with quick difference. The mirror image coefficient variety was strong-minded by apply curvature appropriate of smallest amount four-sided figure to the information obtain from 50 descriptions. Curvature appropriate method use unprocessed information to decide a meaning with unnamed coefficients. This method fundamentally second-hand to locate not in the coefficients charge so that the unique information most excellent hysterics the purpose. The principles of the coefficient that are the most excellent built-in lower the chi-square approximation. The chi-square is described as

$$\sum_i \left(\frac{y - y_i}{\sigma_i}\right)^2 \qquad (1.2)$$

Where y is finest fixed charge, y_i is calculated information and σ_i is the average departure estimation of y_i

The manifestation coefficient assortment for complete 12 next stage bin descriptions is strong-minded as depict in Table 1, and the series connected lump ROI is 0.9 to 1.

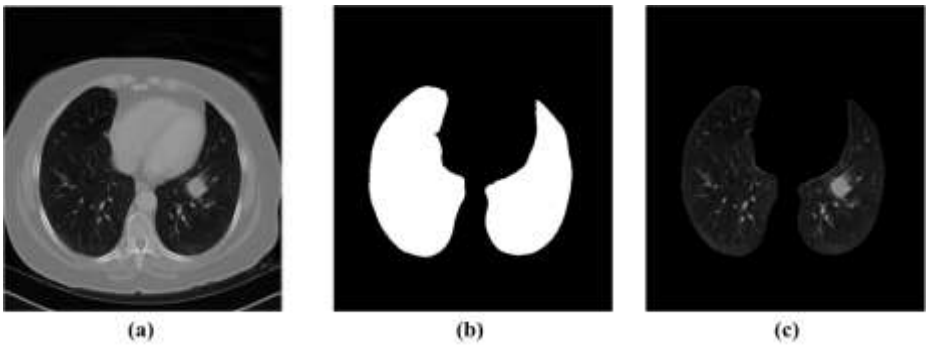

Figure 2. Contribution Lung CT representation with micro-calcification obtain from R_022/analytical Pre-Surgery difference improved CT-97215/2- NONE -69634/000040.dcm (a) Representation extract from Decoma (b) Segmented figure for lung opening (c) Illustration of lung crater with exposed spine enclose.

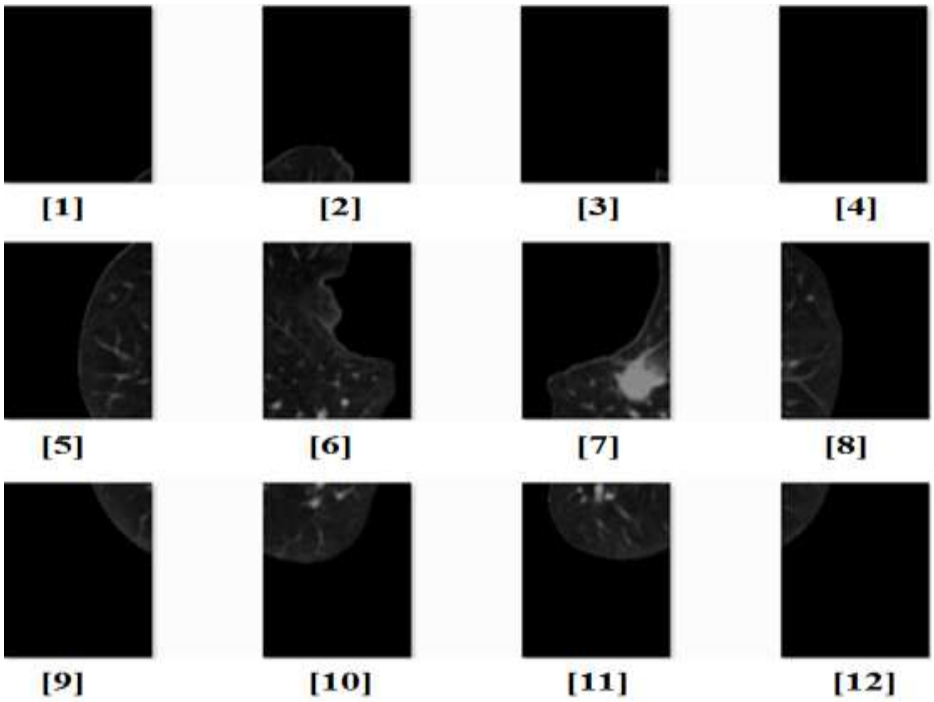

Figure 3. First-level binning of Image (c) given in Figure 2 (bin 7 is subjected to second-level binning)

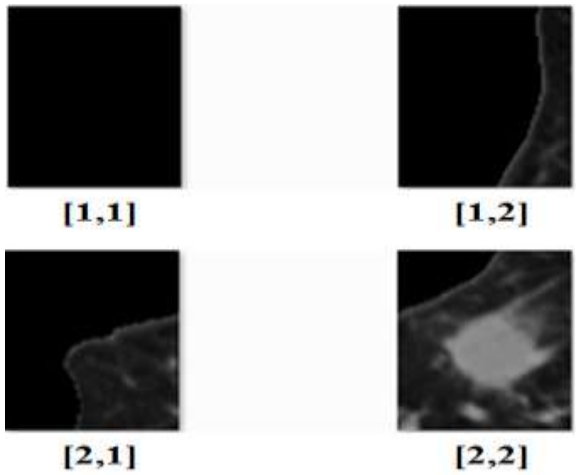

Figure 4. Second-level binning–numbers [1,1]; [1,2]; [2,1]; [2,2]

D. Threshold Segmentation of ROI on the basis of reflection coefficient range

The subdivision of ROI is functional by means of the replication constant series as a edge for detailed charting. The ROI segmented duplicate is consequent (as shown in Figure 12) by means of replication constant choice as a threshold. Then, the balance method of ROI segmented copy that resulting is shared with elected additional equal ditched pictures to effect precise ROI collected the knob relief (as shown in Figure 13). As a result, the ROI is exactly sensed, which might be accessible from sole or extra containers from second-level ditched descriptions.

E. Mass density measurement

The frame thickness is basically a relative by frame each size. Later the node area (micro-calcification) is a calcium statement, the frame thickness of it can be strong-minded. Micro-calcification rises due to the calcium statement explicitly calcium phosphate and calcium oxalate. The calcification of benevolent kind is founded with calcium oxalate while malice kind is of calcium phosphate. The calcium oxalate and of calcium phosphate mass densities are 2.12 g/cm3 and 3.14 g/cm3 individually. The frame of ROI is resolute from pertinent imageries of second-level box by menstruation its individual size. With the unrushed standards, ROI figure thickness is gagged. The appraised figure thickness charge is showed in Table 1.

F. Reflection coefficient and mass density mapping

The figure masses of whole 12 ditched pictures of next equal boxes are strong minded and defined in Table 1, and the spiteful micro-calcified ROI figure mass choice deceits among 2.7 and 3.1 g/cm3. The replication number series that receipts the charge from 0.9 to 1 is plotted to the figure mass that receipts the morals from 2.7 to 3.1 and this presentation is showed in Fig. 10. Later mutually the image numbers and figure masses are strong-minded on the foundation of peel powers in ROI, the relationship among them transpires on lined gage.

Table 1. Measured reflection coefficients, mass densities, and micro-calcification size

Sl. No	Image No	Reflection Coefficients				Mass densities (g/cu.cm)				Micro-calcification Size in mm
		Bin (1,1)	Bin(1,2)	Bin(2,1)	Bin(2,2)	Bin (1,1)	Bin(1,2)	Bin(2,1)	Bin(2,2)	
Malignant Images										
1	1-7	0.2-0.4	0.7-0.8	0.5-0.6	0.9-1	0.88	3.09	2.36	3.65	15.5
2	2-7	0.4-0.5	0.5-0.7	0.4-0.5	0.9-1	1.81	2.54	1.86	3.58	13.7
3	3-7	0.3-0.5	0.5-0.7	0.4-0.5	0.9-1	1.24	2.63	1.82	3.69	12.4
4	4-11	0.9-1	0.5-0.6	0.2-0.4	0.5-0.6	3.74	2.46	1.09	2.52	14.7
5	5-7	0.2-0.4	0.5-0.6	0.6-0.8	0.9-1	0.94	2.61	2.43	3.72	9.5
6	6-7	0.2-0.4	0.6-0.7	0.7-0.8	0.9-1	0.96	2.44	3.56	3.81	14.6
7	7-6	0.6-0.7	0.2-0.3	0.9-1	0.5-0.7	2.32	0.76	3.94	1.82	12.7
8	8-7	0.2-0.3	0.4-0.5	0.5-0.7	0.9-1	0.81	1.35	1.79	3.76	20.8
9	9-7	0.2-0.3	0.4-0.5	0.4-0.7	0.9-1	0.78	1.42	1.84	3.72	19
10	10-7	0.2-0.3	0.4-0.5	0.4-0.6	0.9-1	0.82	1.39	1.76	3.82	29.8
11	11-6	0.6-0.8	0.6-0.8	0.6-0.8	0.9-1	2.15	2.46	2.57	3.86	15.1
12	12-7	0.2-0.3	0.4-0.5	0.5-0.7	0.9-1	0.91	1.43	1.94	3.78	24.8
Normal Images										
13	13-6	0.2-0.3	0.3-0.4	0.6-0.8	0.5-0.7	0.84	1.18	2.89	2.76	0
14	14-8	0.3-0.4	0.5-0.7	0.2-0.3	0.6-0.8	1.27	2.74	0.85	3.21	0
15	15-11	0.5-0.7	0.6-0.8	0.2-0.3	0.3-0.4	1.98	3.02	0.92	1.15	0
16	16-9	0.6-0.8	0.3-0.4	0.5-0.7	0.2-0.3	3.12	1.23	2.38	0.89	0

G. Micro-calcification Pattern Detection and its 3D projection

On the source of the assessed image factor choice and conforming frame thickness of micro-calcification, its decoration on container duplicate is branded, and the resultant shape is signified in 3D forecasts [40].

Plan of the micro-calcified ROI (i) by attractive x and y machetes as the peel rackets and pillars of ditched twin from another equal ditching (64 × 84) and z bloc as assessed image number choice. This is showed in Fig. 17. Revolving 3D predictable ROI to any approach is added valuable for the docs to transmit obtainable scientific inspection decoratively added. This 3D forecast aids to regulate the situation and extent of micro-calcified ROI

H. Determination of micro-calcification size

Meanwhile the 3D forecast of the discarded duplicate can be accomplished in relations of the detachment; the ROI extent is handily appraised. In Fig.4, the x and y machetes are showed as the size and elevation of the discarded duplicate and it establishes a collection of the micro-calcification. A great extent micro-calcified ROI is observed. The powerful straight ROI are perceived, and this section is probable onto x league to harvest the micro-calcified extent and figure. Sl. No 3 in Table 1 shows the extent. The micro-calcified extent changes from the choice of millimeters to a scarce centimeters founded on tumor evolution.

The technique of Interruption guesses the facts at indefinite facts from identified national facts ideas. It is firm to trace careful location of micro-calcification in CT descriptions by filmic. The duplicate fair offers the data on concentrations on the foundation of the flora of lung matter. The found CT duplicate when on leaden gauge adaptation, the concentrations possible to fluctuate among 0 and 255. By means of these statistics and the standards of likeness constant and figure thickness, the scope of hateful micro-calcification is intended perhaps from the design in 3D estimate.

I. Calculating tissue impedance

The matter resistivities are designed from replication constants using calculation (1.3). The Figure 9 and 10 portrays the scheme of material resistances for the line no. 30, 42-47 and 60 of Double 9-7-(2, 2) assumed in Sl. No 3 of Table 1.

$$\Gamma = \frac{Z_L - Z_O}{Z_L + Z_O} \qquad (1.3)$$

In which Γ is image constant, Z_0 is inflight resistivity which is 376Ω and Z_L is the material resistance.

III. Experiment Results and Inferences

The outcomes that track are deliberated in abridged method. Figure 2 (c) is a contribution duplicate. The initial near ditched descriptions of 12 in quantity are showed in Figure 3 with 3 wins and 4 posts. The 7th ditched duplicate contains micro-calcified ROI. Hence, this sixth twin is measured for another equal ditching and the outcomes of another equal ditching are showed in Figure 4 and box [2, 2] contained the micro-calcification lump. This box is elected for extra examination. This box has the extent of 64 × 84. Then, the replication constants are appraised for complete peels connected to box [2, 2]. Additional, the variations in replication constants are graphed for each racket of box [2, 2] and these are showed in Figure. 5 and 6. It is clear from the diagrams that the replication constant differs from 0.9 to 1 from racket 42 till racket 47 for convinced choice of support peels. The considerable variations in likeness constant are highlighted with stripe in red, and the likeness constant variety relating to ROI that strong minded using bend right process of minimum four-sided bend is exposed with stroke in blue. The bend right technique of minimum four-sided diminishes the great variations of replication constants in ROI. The lined relative among the replication constants and frame masses is showed in Figure 7.

The figure thickness standards of entire 4th another equal ditched descriptions are showed in Figure 8, and by this chart and from Table 1, bin [2, 2] has major frame concentration cost. Segmented ROI that exposed in Figure 11 (a) measured the image factor series as a dawn. Figure 11 (b) displays right ROI that charted from Figure 11 (a) for bin [2, 2]. Figure 12 and 13 display the probable 3D twin of sensed micro-calcified ROI design that is supportive to expect their structures. Figure 13 (b) shows micro-calcified area in scope founded on corporal extents.

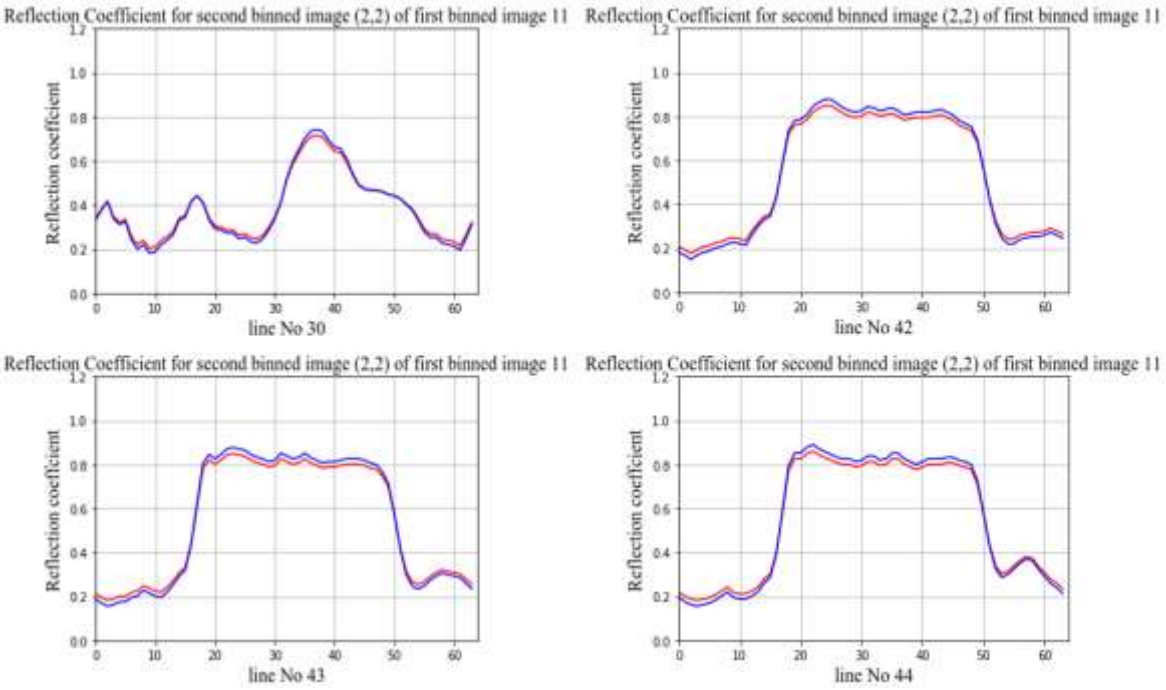

Figure 5. Reflection coefficient plot for bin [2, 2] with row nos. 30 and 42–44

A numerical examination of Lung CT on the base of overhead deliberated process as recommended method, the replication constants and frame masses standards of discarded descriptions from second-level, and the scope of micro-calcification are projected by means of constants projected from 100 imageries with menace. However, the standards those found are charted in Table 1 impartial for 12 tested hateful descriptions and 4 usual descriptions. Table 1 comprises 4 foremost posts, such as double amount, replication constants, frame concentration standards, and scopes of micro-calcified node. The post of duplicate amount post delivers box facts around the double with the individual ampule quantity observed for examination and the pilaster of the box amount delivers which primary equal ditched twin has node, and the post of the box quantity(s) delivers which another equal ditched twin has node. In this broadside, the yield facts that resemble to Sl. No. 4 of Table 1, in which the ditched duplicate quantity is 4-11-(1,1). This destined that contribution twin 4 is observed for first-level ditching, and tenth ditched duplicate delimited the lump. So eleventh ditched duplicate of first equal is measured for additional equal ditching, and the occurrence of node is detected in the tenth bin (1,1). In the support of the replication factor, the replication constants of the 4 second-level ditched pictures are figured and numbered. In the similar method, the form concentrations of the 4 next close ditched descriptions are spread in form concentration support of Table 1. Later, the extreme node calcification scope in millimeter (mm) is showed as past post in Table 1.

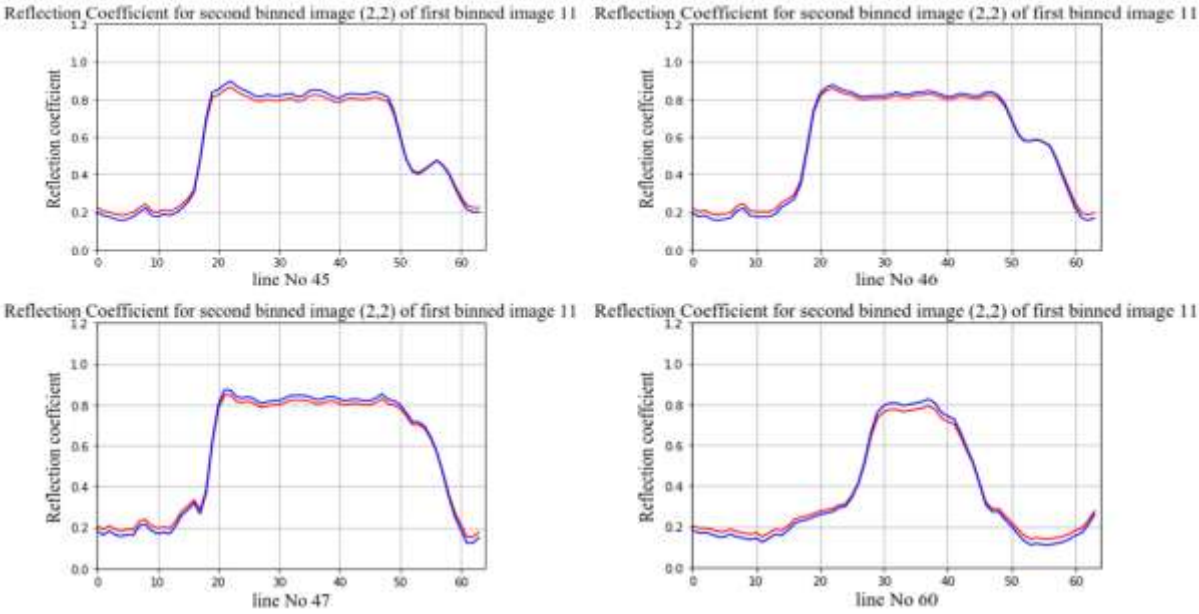

Figure 6. Reflection coefficient plot for bin [2, 2] with row nos. 45-47 and 60

A. Benign and Malign Classification with SVM

100 malevolent and 10 standard descriptions are occupied for the examination now. The presentation of SVM classifier done muddle medium strictures ended 110 imageries is showed in Table 2. The muddle medium limit mostly the correctness is calculated founded on factual optimistic, untrue optimistic, factual undesirable and untrue bad and it is labeled in Figure 14.

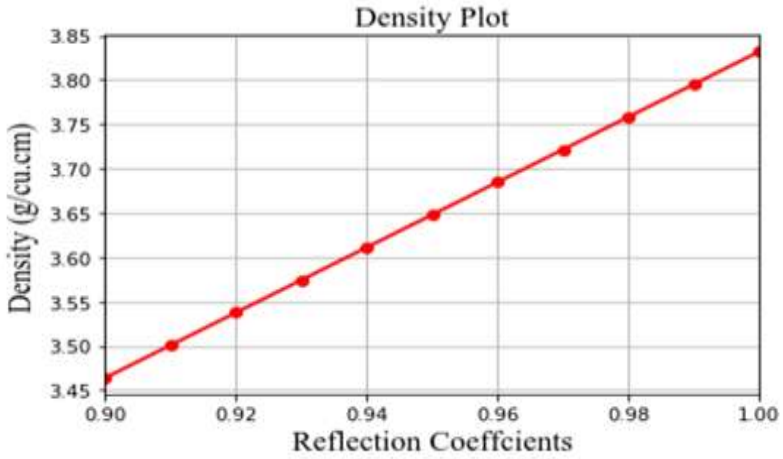

Figure 7. Reflection coefficient and mass density mapping

B. Analysis

From Table 1, it is clearly apparent that the replication constants and frame concentrations of the observed ditched twin will decrease inside the quantified choice. Thus, it is fairly relaxed to expect lump extent accurately. When the facts of Sl. No. 9 measured, the ROI of the box (2, 2) has its replication constant inside the series from 0.9 to 1 and frame concentration in the choice from 1.42 to 3.72 g/cu.cm. For the break of ditched descriptions, the replication constants whitethorn non fib inside quantified series, though their frame thickness standards drop inside quantified choice. Hereafter, the procedure desires the box (2, 2) as ROI departure respite of the boxes. But the duplicate that measured in Sl. No. 9 is an irregularity duplicate; the ROI sensed is in the box (2, 2). In wrong undesirable session, the replication constant and frame concentration of irregularity duplicate might fib in stated choice, the node extent might develop undecided. This is owing to the lung CT duplicate drive take solid frame. The usual CT descriptions might possible to fit factual adverse period. It is understood from figured frame concentrations that the node existing in irregularity descriptions will be of calcium phosphate. On arrangement of duplicate among benevolent and malevolent from corporal structures, the exactness of the

classifier is reached 99%. On comparison with the dominant classifiers, the recommended method which customs Support Vector Machine (SVM) donated a brilliant precision via fair smearing dual chief corporeal structures got from CT pictures. The grades that realized can be offered to the medics for authentication. The proposed way exposed that it is far extra effective and actual in contrast with extra dominant currently present ordering devices. The present mechanism erudition classifiers work on the root by means of resultant structures of data and surfaces. Separately expecting the scope, the recommended procedure completes as a brilliant classifier via with objective dual key corporal structures.

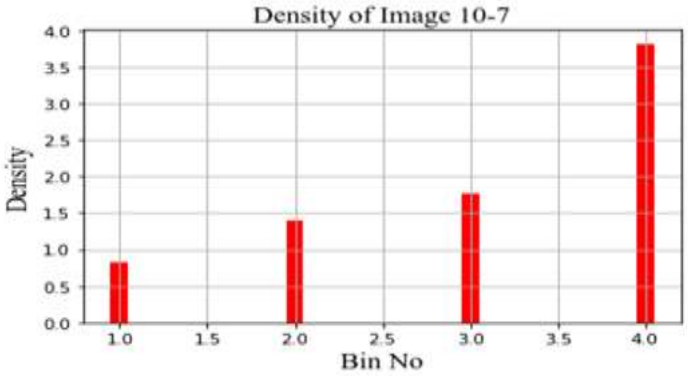

Figure 8. Density calculation of second-level bins

IV. CONCLUSION

This examination optional a novel mechanization technique with CAD process that is to say bin, calculation of the mirror image coefficients and gathering density to draw from a 3D protuberance of lump prototype from lung CT descriptions. In segmenting the lump productively, thresholding on the foundation of the mirror image coefficient was performing. Furthermore, by means of accumulation thickness principles, the kind of calcium drop in the lung can be strong-minded. The calculation of protuberance dimension was approved not by means of exclamation in excess of representation concentration and the mirror image coefficient. Present from, the lump was accurately recognized by means of 3D protuberance of it, and thus its dimension was precisely detected. The gratitude technique practical for examination intended majorly by means of corporeal facial appearance that is mirror image coefficient and collection compactness. Therefore this technique is exclusive, and has been unapplied or unaffected lengthily in a few of former research. The forecast stuck between usual and growth throughout categorization achieves the correctness with 98%. For that reason, the optional technique is established as a well-organized method for diagnose and categorization of the lung malignancy. The 3D protuberance of lump is a suitable graphical demonstration, which is so simple to understand the lump dimension and figure by health center, radiologists and patients.

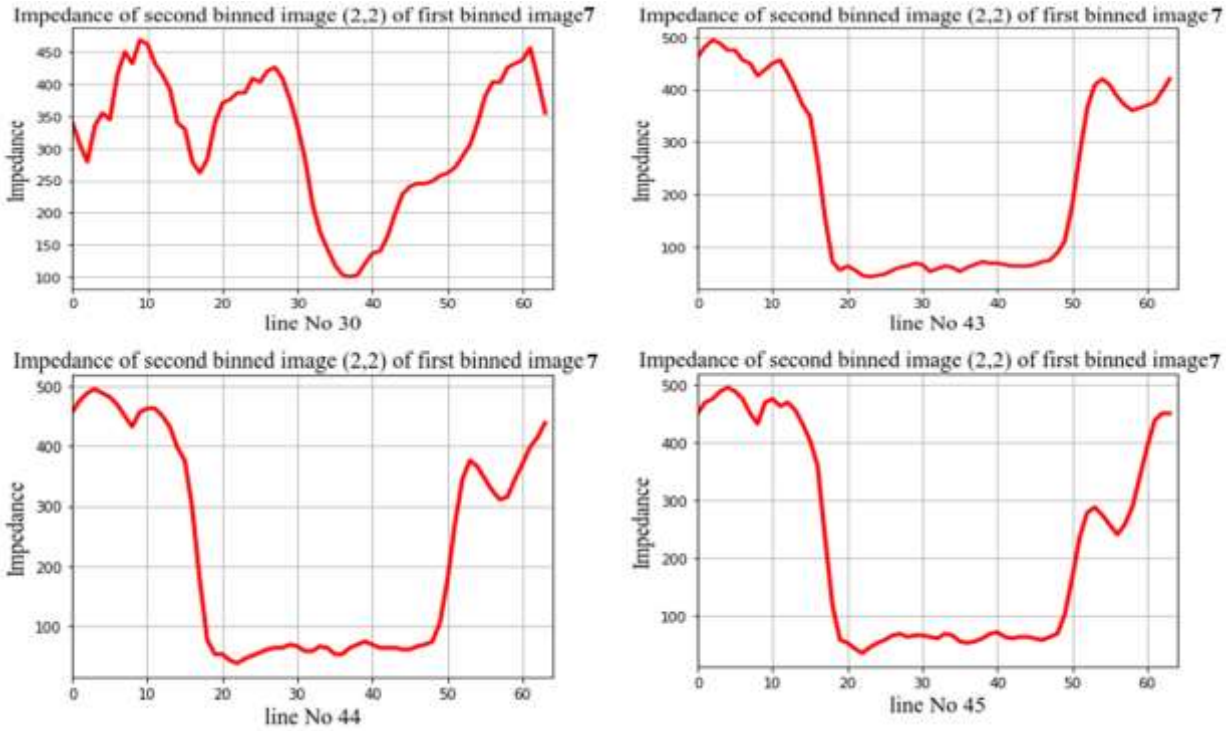

Figure 9. Light Transmission Impedance plot for bin [2, 2] with row nos. 30 and 42–44

0
s

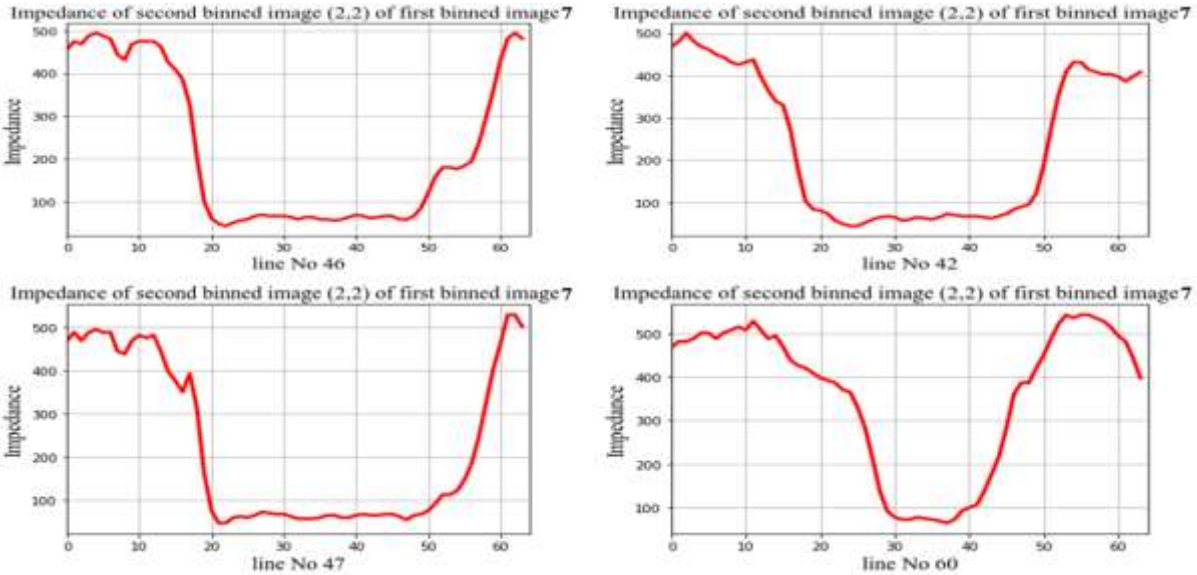

Figure 10. Light Transmission Impedance plot for bin [2, 2] with row nos. 45-47 and 60

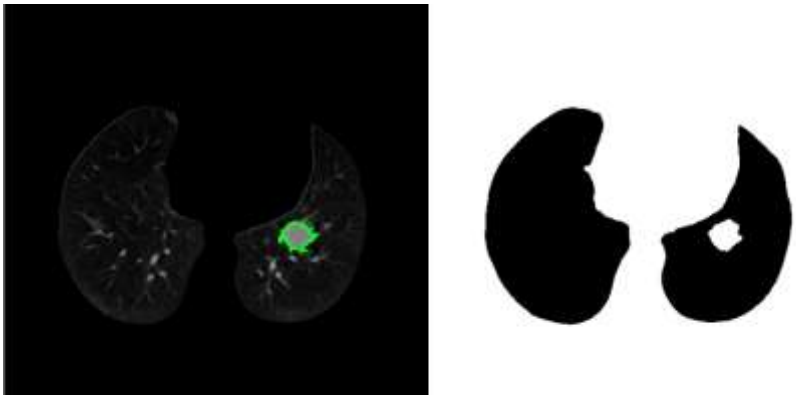

Figure 11. (a)Exact ROI by mapping (b) identifying the ROI by thresholding

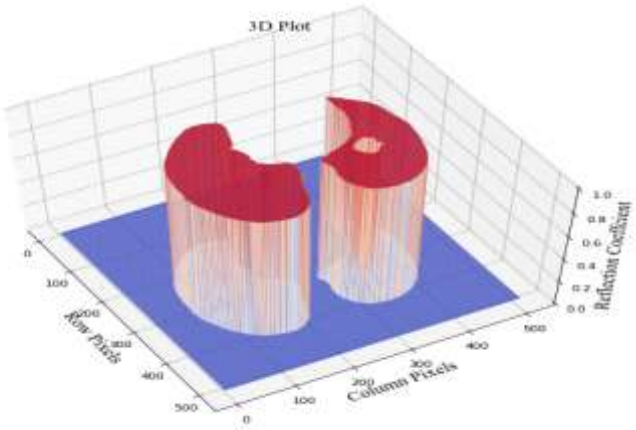

Figure 12. 3D Detection of the micro-calcification pattern for bin [2, 2]

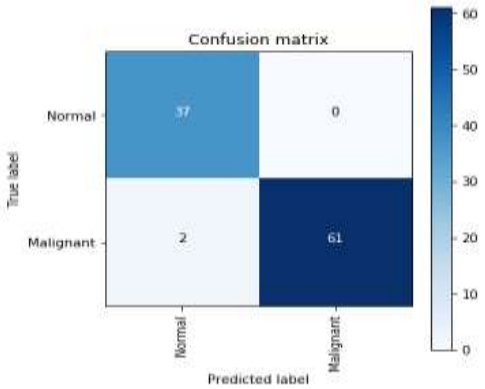

Figure 13. Confusion Matrix of SVM Classifier

Table 2: Prediction Result of SVM Classifier

```
-----------------------------------------------------------
Number of Normal Images in Test    37
Number of Malignant Images in Test 63
Number of Normal Images in Train    57
Number of Malignant Images in Train 65
Number of Normal Images Predicted    39
Number of Malignant Images Predicted 61
True Positive:Normal     37
True Positive:Malignant  61
False Positive:Normal    2
False Positive:Malignant 0
True Negative:Normal     61
True Negative:Malignant  37
False Negative:Normal    0
False Negative:Malignant 2
Sensitivity, Hit Rate, Recall:Normal    100.0
Sensitivity, Hit Rate, Recall:Malignant 96.82539682539682
Specificity:Normal    96.82539682539682
Specificity:Malignant 100.0
Precision or Positive Predictive Value:Normal    94.87179487179486
Precision or Positive Predictive Value:Malignant 100.0
Accuracy:Normal    98.0
Accuracy:Malignant 98.0
```

REFERENCES

1. Media report (ICMR IN NEWS)", Indian Council of Medical Research Department of Health Research – Ministry of Health & Family Welfare Government of India, (2 February to 8 February 2019)

2. Bach P B, Mirkin J N, Oliver T K, Azzoli C G, Berry D A, Brawley O W, Byers T, Colditz G A, Gould M K, Jett J R et al, "Benefits and harms of CT screening for lung cancer a systematic review", J. Am. Med. Assoc. 3072418–29, 2012
3. Siegel R L, Miller K D, Jemal A, "Cancer statistics", *CA Cancer J. Clin.* 68 7–30, 2018
4. Aberle D R, Adams A M, Berg C D, Black W C, Clapp J D, Fagerstrom R M, Gareen I F, Gatsonis C, Marcus P M, Sicks J D, "Reduced lung-cancer mortality with low-dose computed tomographic screening", *New Engl. J. Med.* 365 395–409, 2011
5. Gould M K, Maclean C C, Kuschner W G, Rydzak C E, Owens D K, "Accuracy of positron emission tomography for diagnosis of pulmonary nodules and mass lesions—a meta-analysis", J. Am. Med. Assoc. 285 914–24, 2001
6. Cao P, Liu X L, Yang J Z, Zhao D Z, Li W, Huang M, Zaiane O, "A multi-kernel based framework for heterogeneous feature selection and over-sampling for computer-aided detection of pulmonary nodules", Pattern Recogn. 64 327–46, 2017
7. Ng Q S and Goh V, "Angiogenesis in non-small cell lung cancer imaging with perfusion computed tomography", J. Thorac Imaging25 142–50, 2010
8. Gibaldi A, Barone D, Gavelli G, Malavasi S and Bevilacqua A, "Effects of guided random sampling of TCCs on blood flow values in CT perfusion studies of lung tumors", Acad. Radiol. 22 58–69, 2015
9. Naidich DP, Rusinek H, McGuinness G, et al. "Variables affecting pulmonary nodule detection with computed tomography: evaluation with three-dimensional computer simulation", J Thorac Imaging, 8:291-9, 1993
10. Rubin GD, "Lung nodule and cancer detection in computed tomography screening", J Thorac Imaging, 30:130-8, 2015
11. Gruden JF, Ouanounou S, Tigges S, et al, "Incremental benefit of maximum-intensity-projection images on observer detection of small pulmonary nodules revealed by multi-detector CT", AJR Am J Roentgenol, 179:149-57, 2002
12. Swensen SJ, Jett JR, Sloan JA, et al, "Screening for lung cancer with low-dose spiral computed tomography. Am J RespirCrit Care Med", 165:508-13, 2002
13. van Klaveren RV, Oudkerk M, Mali W, et al, "Baseline and second round results from the population based Dutch-Belgian randomized lung cancer screening trial (NELSON)", J ClinOncol 26:1508, 2008
14. National Lung Screening Trial Research T, Aberle DR, Adams AM, et al, "Reduced lung-cancer mortality with low-dose computed tomographic screening", N Engl J Med, 365:395-409, 2011
15. Moyer VA, "U.S. Preventive Services Task Force. Screening for lung cancer: U.S. Preventive Services Task Force recommendation statement", Ann Intern Med 160:330-8, 2014
16. W. Wang, S. Wu, "A Study on Lung Cancer Detection by Image Processing", International Conference on Communications, Circuits and Systems, ICCCAS, Proceedings, 2006
17. Veerakumar K., Ravichandran C.G. "Intensity, Shape and Size Based Detection of Lung Nodules from CT Images", In: Prasath R., Kathirvalavakumar T. (eds) Mining Intelligence and Knowledge Exploration. Lecture Notes in Computer Science, Vol 8284. Springer, Cham, 2013
18. Neelima.S, A. Asuntha "Image Processing used for Lung Cancer Detection in Medical Imaging", Journal of Chemical and Pharmaceutical Research, 8(4):1044-1049, 2016
19. S. Indira Priyadharsini, N. Mangayarkarasi, L. SaiRamesh, G. Raghuraman, "Lung nodule detection on CT images using image processing techniques", International Journal of Pure and Applied Mathematics, Vol. 119 No. 7, 479-487, 2018
20. Dr.G.R.Jothi lakshmi.,Dr. Arun Raaza , Dr. Y. Sreenivasa Varma , Dr. V. Rajendran , R. Guru Nirmal Raj 2018 ,"A review of characteristic study of micro calcification using son mammogram images", International Journal of Engineering & Technology, 7 (2.33) (2018) 290-294
21. Dr.G.R.Jothi lakshmi., E. Gopinathan 2015 "Mamogram enhancement using quadratic adaptive volterra filter- A comparative analysis in spatial and frequency domain",ARPN Journal of Engineering and Applied Sciences